Association Aéronautique et Astronautique de France

56th 3AF International Conference on Applied Aerodynamics
28 — 30 March 2022, Toulouse – France

FP14-AERO2022-videlier

Simulation of the effect of a vertical gust on the flow around a thin airfoil by dicrete vortex method

Vincent Videlier[(1)] and Thierry M. Faure[(2)]
Ecole de l'Air et de l'Espace, Centre de Recherche de l'Ecole de l'Air F-13661 Salon air France
[(1)]vincent.videlier@ecole-air.fr
[(2)]thierry.faure@ecole-air.fr

ABSTRACT

The thin airfoil theory is reviewed pointing there is no impediment considering a thin airfoil in a non-uniform flowfield. This can be worked on by the Leading-edge-suction-parameter modulated Discrete Vortex Method (LDVM) to obtain an accurate unsteady solution, at low Reynolds number, when the flow is detached. Considering the example of the aerodynamic response of a flat plate encountering a large amplitude sharp-edged gust, we compare predictions from this method with the reference theory, simulations results and the experimental data from literature.

1. INTRODUCTION

Thin airfoil theories have always been worked on assuming a known far-field steady velocity relative to the airfoil. Under this assumption, kinematics are added to the airfoil and generates an unsteady local velocity relative to the air flow. Distributed electric propulsion of Unmanned Air Vehicles (UAV) with Vertical Take-Off and Landing (VTOL) capabilities emphasize the necessity to overcome the classical upstream velocity and angle of attack (U_∞, α) formulation, it is needed to predict wing response in complex airflow resulting from the propellers wake, typically in hover configuration, where (U_∞, α) are not clearly defined. It is possible to change the concept of free steam velocity when it is small or zero on the far field and replace it with the velocity at the leading edge (velocity is then generated by the input kinematics), to still be able to solve the approach, as in [8]. But these methods are limited to realistic kinematics and non-velocity-nullifying motions.

The modification of the thin airfoil theory for non-uniform airflow would not provide an accurate solution of the observed behavior, because of the non-uniformity happening at low Reynolds number when the flow is detached. In these situations potential solutions with simplified wakes do not match very well with the experiments. For this reason this issue is of particular interest using reduced order methods like the LDVM [7]. The wing-gust encounter case is chosen to illustrate this paper because it is well documented and shows clearly the differences we want to highlight on the method used to model the velocity field.

2. THIN AIRFOIL THEORY WITH GENERAL NON UNIFORM FLOWFIELD

In this section, we adapt the thin airfoil theory so it can be used with a non uniform flowfield. The airfoil is modeled with the classical continuous vorticity line along the chord. The flowfield is described as:

$$\overrightarrow{U} = u_x(x,z,t)\overrightarrow{x} + u_z(x,z,t)\overrightarrow{z} \tag{1}$$

with $(u_x; u_z)$ the velocity components along the axes and $\overrightarrow{U}$ the velocity vector. The airfoil is defined by function $z_c(x)$ which is the camberline of the airfoil. With the hypothesis of the thin airfoil theory that $\mathrm{d}z_c/\mathrm{d}x \ll 1$, the normal velocity w to the airfoil is evaluated along the chordwise direction by :

$$w(x) = u_z(x,0) - \frac{\mathrm{d}z_c}{\mathrm{d}x} u_x(x,0) \tag{2}$$

The normal velocity component is linked to the chordwise vorticity distribution $\gamma(x)$ by considering a zero normal flow through the chord of the airfoil:

$$w(x) = \frac{1}{2\pi}\int_0^c \frac{\gamma(x^*)}{x-x^*}\mathrm{d}x^* \tag{3}$$

with c the airfoil chord. The thin airfoil fundamental equation becomes :

$$\frac{\mathrm{d}z_c}{\mathrm{d}x}u_x(x) - u_z(x) = \frac{-1}{2\pi}\int_0^c \frac{\gamma(x^*)}{x-x^*}\mathrm{d}x^* \tag{4}$$

$$W(x) = \frac{\mathrm{d}z_c}{\mathrm{d}x}u_x - u_z \tag{5}$$

with the following vorticity distribution:

$$x = \frac{c}{2}(1-\cos(\theta)) \tag{6}$$

$$\gamma(\theta) = 2(A_0\frac{1+\cos(\theta)}{\sin(\theta)} + \sum_{n=1}^{\infty} A_n \sin(n\theta)) \tag{7}$$

with the expressions of the Fourier coefficients A_n:

$$A_0 = \frac{-1}{\pi}\int_0^{\pi} W(\theta)d\theta \tag{8}$$

$$A_n = \frac{2}{\pi}\int_0^{\pi} W(\theta)\cos(n\theta)d\theta \tag{9}$$

Note that these expressions are dimensional and does not involve any reference velocity.

2.1 Forces and moments

Using Bernouilli unsteady equation as in [4][7] the local pressure difference is evaluated:

$$\Delta p(x) = \rho\left[\frac{1}{2}(V_{xup}^2 - V_{xlow}^2) + \frac{\partial\phi}{\partial t}_{up} - \frac{\partial\phi}{\partial t}_{low}\right] \tag{10}$$

Since there is no global relative speed between the airfoil and its environment, the local sum of the perturbations and the wake is evaluated. Let $T(x)$ be the expression of all the flow contributions to the tangential velocity, then :

$$\frac{1}{2}(V_{tup}^2 - V_{tlow}^2) = T(x)\gamma(x) \tag{11}$$

$$\frac{\partial\phi}{\partial t}_{up} - \frac{\partial\phi}{\partial t}_{low} = \frac{\partial}{\partial t}\int_0^x \gamma(x) \tag{12}$$

$$\Delta p(x) = \rho\left[T(x)\gamma(x) + \frac{\partial}{\partial t}\int_0^x \gamma(x)\right] \tag{13}$$

$$F_N = \rho\left[\int_0^c T(x)\gamma(x)\mathrm{d}x + \int_0^c \frac{\partial}{\partial t}\int_0^x \gamma(x)\mathrm{d}x\right] \tag{14}$$

with F_N being the normal force on the airfoil. $V_{t_{up}}$ and $V_{t_{low}}$ being the tangential velocity respectively on the top and on the bottom of the airfoil and ϕ being the velocity potential associated with the bound vorticity, ρ is the density of the fluid. The second part will be evaluated using dimensional Fourier coefficients from the previously described non-uniform thin airfoil theory. However, it is not possible to separate the first integral as it was done in [4][7]. The normal force is reduced to :

$$F_N = \rho\pi c\left[\int_0^c T(x)\gamma(x)dx + \frac{c}{4}(3\dot{A_0} + \dot{A_1} + \frac{1}{2}\dot{A_2})\right] \tag{15}$$

The leading-edge suction force acting axially on the aerofoil is:

$$F_S = \rho\pi c A_0^2 \tag{16}$$

The pitching moment relative to the pivot x_0 coordinate, can be evaluated similarly with the $T(x)$ function from:

$$M = \int_0^c \Delta p(x_0 - x)\mathrm{d}x \tag{17}$$

Note that we cannot evaluate the aerodynamic coefficient due to the lack of a proper definition of the upstream flow speed U_∞. Then, we propose to use the local airspeed velocity on the chord $U(x)$ leading to:

$$C_L = \frac{L}{\frac{1}{2}\int_0^c \rho U(x)^2\mathrm{d}x} \tag{18}$$

$$C_M = \frac{M}{\frac{c}{2}\int_0^c \rho U(x)^2\mathrm{d}x} \tag{19}$$

3. NON-UNIFORM LDVM

In this section, we extend the LDVM from [7] to a non-uniform airflow, referred as LDVMNU standing for LDVM Non-Uniform. Firstly, the angle-of-attack α is no longer defined relatively to the free stream velocity U_∞ but from the angle bewteen the geometric reference frame (X,Z) and the (x,z) frame that is attached and defined from the airfoil leading and trailing edge; as shown in Fig. 1. $h(t)$ is the vertical motion along Z.

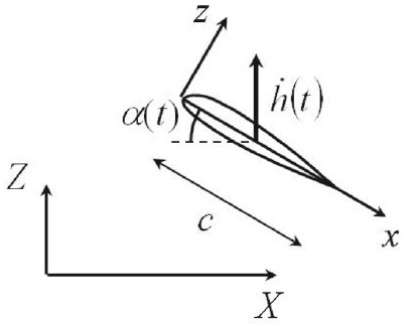

Figure 1: Airfoil and frames of reference

An external velocity field is superimposed, to all the velocity input. The external velocity field can be either represented by the $U(x,z,t)$ function or by a series of discrete vortices. In the present paper, an analytical approach is used to construct the vortex series. The downwash becomes:

$$W(x,t) = \frac{\partial \eta}{\partial x}\left[U_x(x,t)\cos\alpha - U_z(x,t)\sin\alpha + \dot{h}\sin\alpha + \frac{\partial \phi_{init}}{\partial x} + \frac{\partial \phi_{lev}}{\partial x} + \frac{\partial \phi_{tev}}{\partial x}\right] - U_x(x,t)\sin\alpha - U_z(x,t)\cos\alpha - \dot{\alpha}(x-x_0) + \dot{h}\cos\alpha - \frac{\partial \phi_{init}}{\partial x} - \frac{\partial \phi_{lev}}{\partial z} - \frac{\partial \phi_{tev}}{\partial z} \quad (20)$$

where ϕ_{init} is the velocity potential associated with the series of discrete vortex modeling the initial external velocity field. ϕ_{lev} and ϕ_{tev} are the velocity potential associated with the leading and the trailing edge vortices, η is the airfoil camberline and x_0 the position of the $\dot{\alpha}$ pivot point.

The Leading-Edge Suction Parameter (LESP) is defined by [7] as a non-dimensional measure of the suction at the leading edge and is shown equal to the A_0 coefficient. Following the work of [8], the LESP is divided at each time step with the local velocity at the leading edge which results from every external contributions.

$$LESP(t) = \frac{A_0(t)}{V_{mag}(t)} \quad (21)$$

Where V_{mag} is the local leading-edge velocity that result from the contributions of the freesteam velocity, the initial discrete vortex series, the leading edge and trailing edge vortices and the relative speed generated by the airfoil's motion. The critical $LESP$, $LESP_{crit}$, is the threshold corresponding to a leading edge detachment, modeled by a leading edge vortex shedding. This $LESP_{crit}$ can be, depending on the intensity of the non uniformity, evaluated on each time step according to the leading-edge local velocity as done in [8].

4. WING-GUST INTERACTION SOLUTION

4.1 Vertical gust model

Following the approach of [2], the gust is modeled by two infinite vortex lines of constant and opposite vorticity as shown in Fig. 2. From this model we can approach the two shear layers with N vortices, distributed along each layer spaced by a distance D throughout a height h. We define δ as the number of vortex per chord length unit. It is also common to define the gust ratio GR as the intensity of the gust relative to the free-steam velocity (Eq. 22). The circulation of each vortex is then given by Eq. 23.

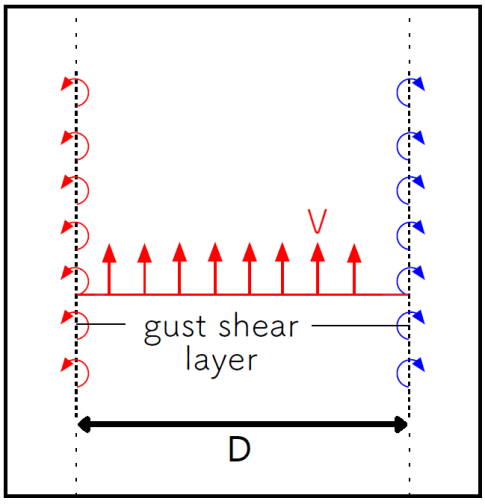

Figure 2: Gust model from [2]

The velocity field generated by this model is shown in Fig. 3

$$GR = \frac{V}{U_\infty} \quad (22)$$

$$\Gamma = GR \cdot \frac{h}{N} \quad (23)$$

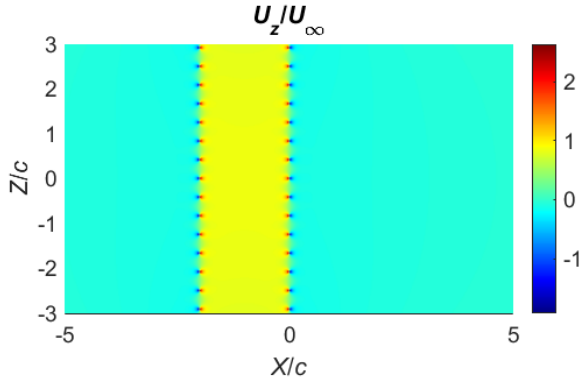

Figure 3: Velocity field generated for a gust with D/c = 2, GR = 1, h/c = 25 and δ = 2.5

4.2 Results

The current configuration considers a relative gust length $D/c = 2$ with a relative total height $h/c = 50$. The vortex density δ is set to 2.5 vortex per chord. The lift coefficient C_L is presented considering the non-dimensional time t^* (Eq. 24).

$$t^* = t\frac{U_\infty}{c} \quad (24)$$

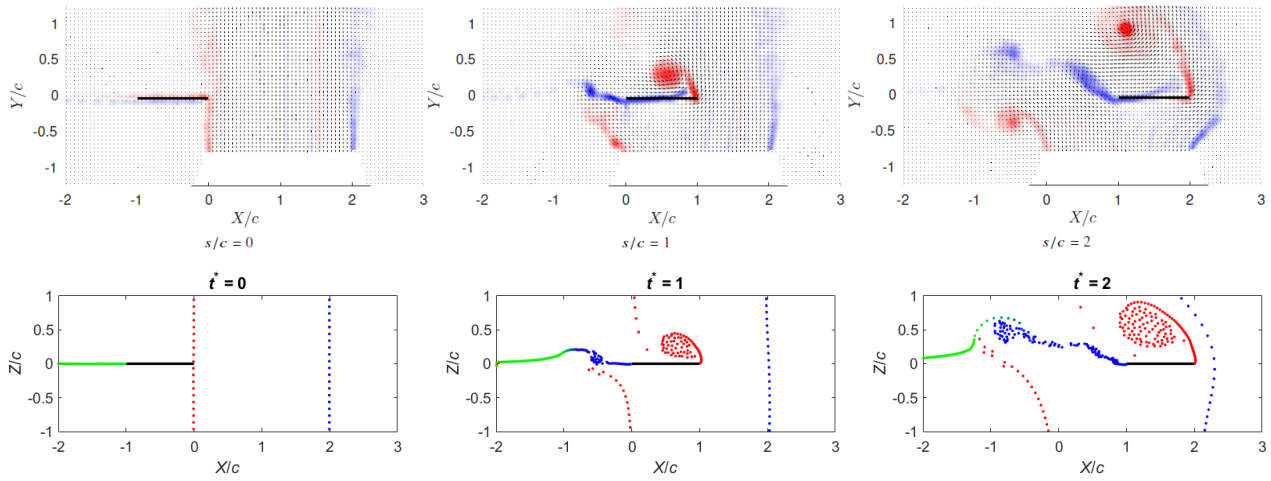

Figure 4: Qualitative comparison of the reference case simulated in LDVMNU with PIV measurements from [3]

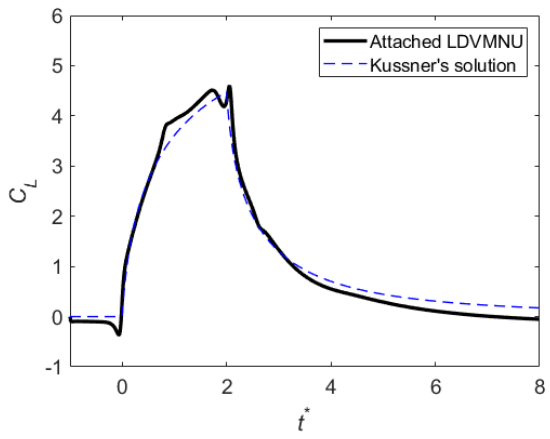

Figure 5: Attached LDVMNU wing-gust interaction

Unless specified, the values used in the present paper are those of the reference case. The intended behavior is confirmed by a simulation that is carried out with an attached flow, obtained by enforcing $LESP_{crit}$ to a very high value. The results are presented in Fig.5 and agree well with the reference theory (Kussner's solution). Concerning detached flows, simulations extracts can be found in Fig. 4 and are also in agreement with the experiment. The deformation of the shear layers is well represented. Note that in the experiment, the gust is generated using a duct under the wing limiting the deformation of the shear layers.

4.2.1 Modelled height influence

The influence of the length of the modelled shear layer on the results is considered varying h/c in Fig. 6. Little difference is found for t^* between 0 and 2.5, considering $h/c = 50$ or 1000. For the lower value 10, the simulations are diverging as the shear layers are unable to accurately model the top-hat velocity profile. The latter values (from $t^* > 2.5$ in this figure), are rejected because of a complex that forms from this point, see Section. 4.2.4. Higher values are not found to significantly improve the accuracy of the results.

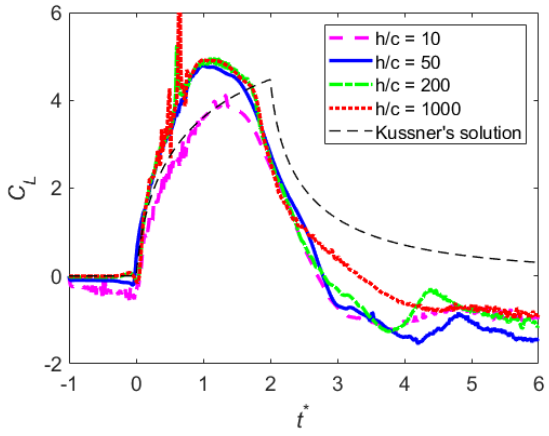

Figure 6: LDVMNU wing-gust interaction for different heights of the vortex lines modeling the gust

4.2.2 Vortex spacing influence

The influence of the vortex density δ is presented in Fig.7. Converging results are observed among the differents values of δ with no apparent impact on the accuracy of the solution. Irregularities starts appearing for lower values of δ as the individual vorticity of each discrete vortex is getting stronger. This is likely due to the local inaccuracy on the prescribed velocity fields. Best

results are obtained with a value of $\delta = 2.5$, this density value being quite far from that prescribed by [6] for the accurate representation of shear layers. Quicker results seems to be obtainable with lower values but then a local smoothing would be recommended.

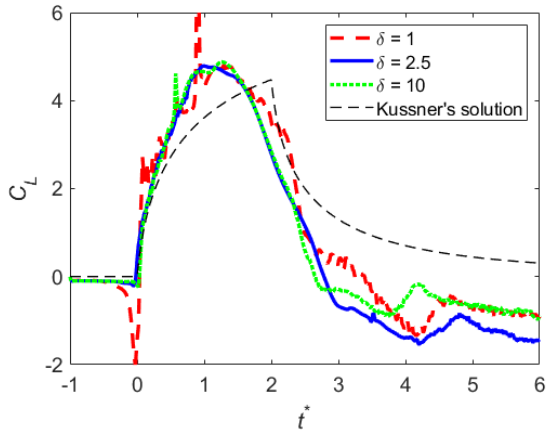

Figure 7: LDVMNU wing-gust interaction for different discrete vortex density in the shear layers

4.2.3 Results for various gust length

To increase gust length it is important to notice the convergence of the velocity field toward the theoretical gust profile, at fixed vortex density δ, is dependant of h/D. The height has to be corrected to obtain similar flowfield accuracy. Therefore results for gust length D/c of 4, 8 and 20 (simulating an impulse response), have their h/c value respectively increased to 100, 200 and 500.

In Fig. 8, a very good agreement is observed with the experiment, both in lift peak value and position, where it seems to outperform results from [1]. From $t^* = 2.5$ the lift prediction of the LDVMNU starts to decrease faster and lower compared to both the experiment and the theory. This is attributed to be the consequence of a stable vortex structure, this phenomenon is further studied in Section 4.2.4. After the exit of the airfoil from the gust, the lift coefficient remains at a value around -1 for the same reason.

Fig.9 shows also a quite good agreement with Badrya's results [1] and the tendency is well reproduced even though oscillations of the lift coefficient are observed. For longer gusts, in Fig.10 and Fig.11, an oscillatory behavior with lift coefficient is also and more present. It oscillates between the theoretical attached flow predictions from the Kussner theory and the asymptotic static stall lift coefficient value predicted in [1]. This is observed to be caused by the periodic shedding of leading-edge and trailing edge vortices into the airfoil wake. It could be explained because the present simulations are

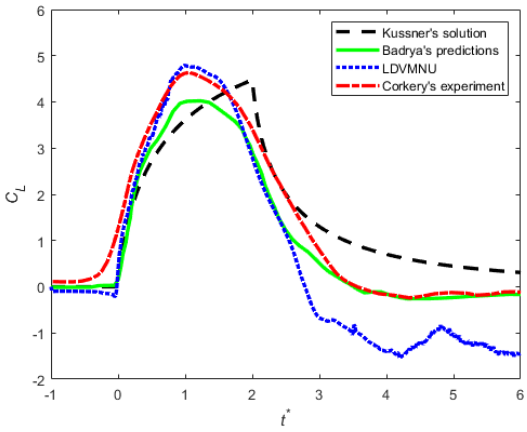

Figure 8: Reference case of LDVMNU, for $h/c = 50$ and $\delta = 2.5$ compared with experiment from [3], with simulations from [1] and reference theory

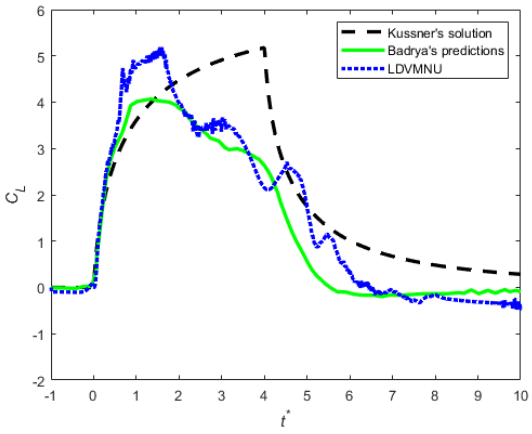

Figure 9: LDVMNU prediction of the encounter of a gust of length $D = 4$ compared with simulations from [1] and reference theory

being carried at a lower Reynolds number -the reason being that the critical LESP is only known for that value- while Badrya's results correspond to a Reynolds number of 40 000. It is also believed that this behavior is a true physical phenomenon.

4.2.4 LDVM and stable structures

The lift coefficient not returning to the expected zero value, even long after the gust interacted with the airfoil, is found to be attributed to a non-physical stable structure forming right after the airfoil exits the gust. The structure is fed by Leading-Edge Vortices stacking close under the airfoil and forming together a high vorticity area. This vorticity complex is inducing enough normal velocity over the airfoil to maintain LEV shedding and self-sustain itself. It is very likely that the structure would

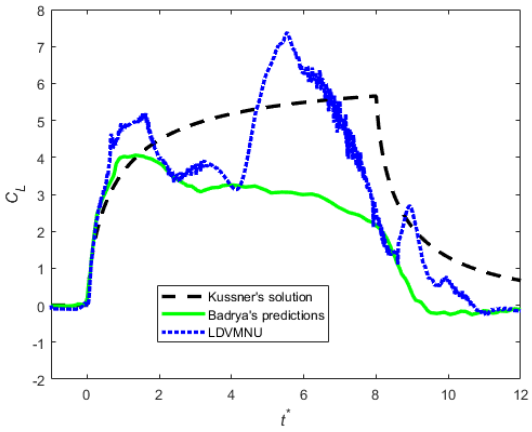

Figure 10: DVMNU prediction of the encounter of a gust of length $D = 8$ compared with simulations from [1] and reference theory

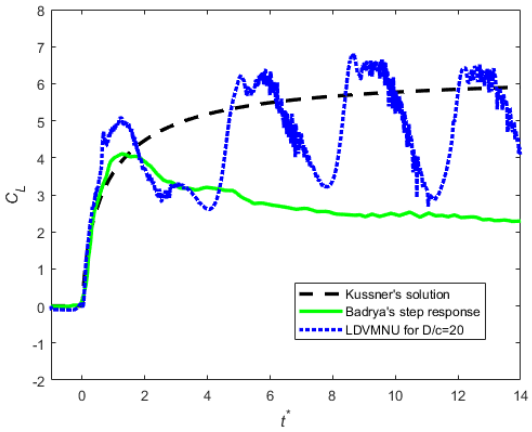

Figure 11: Step gust response compared with simulations from [1] and reference theory

disappear in presence of dissipative effects. The presence of such a structure does not appear to be linked to the current non-uniform variation specifically, but rather to the LDVM. It is likely that similar structures could be encountered with the conventional formulation and uniform motion of the airfoil.

5. CONLCUSION

The current LDVMNU is predicting accurately and rapidly the behavior of an airfoil in a non-uniform flow, modeling a vertical gust, even at low Reynolds and for a completely detached flow. Those features makes it a great candidate in the fast evaluation of performance of hybrid aircraft considering flight transition phases. Even though the computation time of the current simulations is not quick enough to be used easily in parameter exploratory pre-design calculations, it is partialy related to the huge number of discrete vortices needed to model accurately the discontinuous velocity field that is present in the wing-gust interaction problem. It is very likely that almost every other practical velocity field would be represented accurately enough to obtain great result with only a fraction of the vortex needed in this case. On top of that, There is no obstacle for that method to integrate fast summation method or clusterisation of vortices like those developed in [5]. A further step is still to be done to extend theses calculations in three dimensions but it has already been initiated in [4].

REFERENCES

[1] Camli Badrya, Anya R Jones, and James D Baeder. Unsteady aerodynamic response of a flat plate encountering large-amplitude sharp-edged gust. *AIAA Journal*, pages 1–16, 2021.

[2] Simon J Corkery and Holger Babinsky. An investigation into gust shear layer vorticity and the added mass force for a transverse wing-gust encounter. In *AIAA Scitech 2019 Forum*, page 1145, 2019.

[3] Simon James Corkery. *Unsteady aerodynamics of wing-gust encounters*. PhD thesis, University of Cambridge, 2019.

[4] T. M. Faure and C. Leogrande. High angle-of-attack aerodynamics of a straight wing with finite span using a discrete vortex method. *Physics of Fluids*, 32(10):104109, 2020.

[5] Thierry M. Faure, Laurent Dumas, Vincent Drouet, and Olivier Montagnier. A modified discrete-vortex method algorithm with shedding criterion for aerodynamic coefficients prediction at high angle of attack. *Applied Mathematical Modelling*, 69:32 – 46, 2019.

[6] Anthony Leonard. Vortex methods for flow simulation. *Journal of Computational Physics*, 37(3):289–335, 1980.

[7] K. Ramesh, Ashok Gopalarathnam, K. Granlund, M. Ol, and J. R. Edwards. Discrete-vortex method with novel shedding criterion for unsteady aerofoil flows with intermittent leading-edge vortex shedding. *Journal of Fluid Mechanics*, 751:500–538, 2014.

[8] Kiran Kumar Ramesh, Ashok Gopalarathnam, Jack R Edwards, Kenneth O Granlund, and Michael V Ol. Theoretical analysis of perching and hovering maneuvers. In *31st AIAA Applied Aerodynamics Conference*, page 3194, 2013.